Letter

Propagating charge carrier plasmons in Sr_2RuO_4

Martin Knupfer,[1] Fabian Jerzembeck,[2] Naoki Kikugawa,[3] Friedrich Roth,[4,5] and Jörg Fink[1,6]
[1]*Leibniz Institute for Solid State and Materials Research Dresden, Helmholtzstrasse 20, D-01069 Dresden, Germany*
[2]*Max Planck Institute for Chemical Physics of Solids, Nöthnitzer Strasse 40, D-01187 Dresden, Germany*
[3]*National Institute for Materials Science, Tsukuba 305-0003, Japan*
[4]*Institute of Experimental Physics, TU Bergakademie Freiberg, Leipziger Strasse 23, D-09599 Freiberg, Germany*
[5]*Center for Efficient High Temperature Processes and Materials Conversion, TU Bergakademie Freiberg, D-09599 Freiberg, Germany*
[6]*Institut für Festkörperphysik, Technische Universität Dresden, D-01062 Dresden, Germany*

(Received 13 October 2022; accepted 1 December 2022; published 12 December 2022)

We report on studies of charge carrier plasmon excitations in Sr_2RuO_4 by transmission electron energy-loss spectroscopy. In particular, we present results on the plasmon dispersion and its width as a function of momentum transfer. The dispersion can be qualitatively explained in the framework of random phase approximation calculations, using an unrenormalized tight-binding band structure. The constant long-wavelength width of the plasmon indicates that it is caused by a decay into interband transitions and not by quantum critical fluctuations. The results from these studies on a prototypical correlated metal system show that the long-wavelength plasmon excitations near 1 eV are caused by resilient quasiparticles and are not influenced by correlation effects.

DOI: 10.1103/PhysRevB.106.L241103

Introduction. Unconventional superconductors are one of the most active research fields in solid state physics. The reason for this is not only the observed high superconducting transition temperature. These materials also show very often strange normal-state properties. The latter are caused by strong electron-electron interactions leading to correlation effects discussed in the context with quantum critical behavior. The renormalizations of single-particle excitations are described by the complex self-energy Σ, the real and the imaginary part of which are related to the mass renormalization m^*/m and the scattering rate Γ, respectively.

In the doped cuprates, there are numerous studies of single-hole excitations by angle-resolved photoemission spectroscopy (ARPES) providing detailed knowledge of the self-energy yielding a mass renormalization of the conduction band of about two [1]. Furthermore, there are studies of the spin excitations compiled in Ref. [2]. On the other hand, there are only a few studies on momentum-dependent charge degrees of freedom. There is an ongoing discussion, how the renormalization of the single-particle excitations, i.e., the mass renormalization and the finite scattering rate, influences the existence, the dispersion, and the lifetime broadening of two-particle charge excitations (plasmons) in the cuprates.

Several theoretical studies [3–5] have predicted that spin excitations strongly influence the charge excitations. On the other hand, the observation of a continuum instead of the high-energy plasmon was discussed for quantum critical systems based on holographic theories [6], which predicted, different from the classical Landau damping [7], a strong "overdamping" even for the long-wavelength plasmons. These theoretical investigations seem to be supported by electron energy-loss spectroscopy (EELS) in reflection (R-EELS) studies of cuprates [8–10] in which not well-defined propagating plasmons or even only a continuum of excitations were detected. On the other hand, there are EELS studies in transmission (T-EELS) [11–16] on cuprates [17–22] where the dispersion of well-defined plasmons could be explained in terms of collective excitations within an *unrenormalized* band structure.

To better understand the problem, in the present Letter, we extend the studies to Sr_2RuO_4, a highly correlated metal with an even higher average effective mass of about four, using T-EELS. Sr_2RuO_4 is a prototype of unconventional superconductors which shows a Fermi-liquid behavior below 26 K, while at higher temperatures there are deviations from a Fermi liquid violating the Mott-Ioffe-Regel limit [23,24]. The superconducting order parameter is still a matter of controversy [25]. The strongly correlated normal-state electronic structure has been studied by optical spectroscopy [26–30], by R-EELS [31], by tunneling spectroscopy [32], and by ARPES [33–39], in some cases supported by density functional theory (DFT) or combined DFT plus dynamical mean-field theory (DFT+DMFT) calculations [39–41]. The latter two experimental techniques probe essentially one-particle (electron or hole) properties whereas the first two methods probe two-particle excitations (hole plus electrons).

Using slices of the Sr_2RuO_4 crystal cut perpendicular to the **c** axis together with an orientation of the **c** axis parallel to the electron beam, in the present T-EELS measurements, the momentum can be varied within the (**a**, **b**) plane. The momentum parallel to the beam is negligible. Optical spectroscopy measuring excitations with zero momentum transfer [26,27,29,30] found for a photon polarization perpendicular to the **c** axis a well-pronounced plasmon near 1.5 eV with a plasmon width of $\approx$1 eV. For a polarization parallel to the **c** axis, a low-energy plasmon was detected by optical

spectroscopy [26–28]. Moreover, an acoustic plasmon has been detected by R-EELS [31], which was ascribed to a "demon" plasmon on the basis of interacting excitations of heavy and light electrons.

The existence of a high-energy and a low-energy plasmon was already predicted from a calculation of the high in-plane and the low out-of-plane Fermi velocities on the basis of band-structure calculations [40].

The main result of the present Letter is the observation of a well-defined propagating plasmon which in the *nonlocal* long-wavelength limit can be qualitatively explained by random phase approximation (RPA) calculations based on an *unrenormalized* local density approximation (LDA) band structure. This indicates that the low-momentum dispersion is not influenced by the *local* on-site Coulomb interaction. The results also demonstrate that single-hole excitations (measured by ARPES) are much stronger screened than two-particle electron-hole excitations (measured, e.g., by T-EELS).

Experiment. Sr_2RuO_4 crystals were grown using the traveling floating-zone method [42]. The superconducting transition temperature of the sample was $T_c = 1.5$ K. For the EELS measurements, thin films with a thickness of ≈100 nm were cut perpendicular to the crystal **c** axis from these single crystals using an ultramicrotome equipped with a diamond knife. The films were then put onto standard transmission electron microscopy grids and transferred into the spectrometer. The measurements were carried out at a sample temperature of $T = 20$ and 300 K with a dedicated transmission electron energy-loss spectrometer [15,16] employing a primary electron energy of 172 keV. The energy and momentum resolution was set to $\Delta E = 80$ meV and $\Delta q = 0.035$ Å^{-1}, respectively. In all measurements, the momentum transfer was parallel to the (**a**, **b**) plane. Before measuring the loss function, the thin films have been characterized by *in situ* electron diffraction, in order to orient the crystallographic axis with respect to the transferred momentum.

Calculations. For the calculation of the complex dielectric function we used the Ehrenreich-Cohen expression [43,44]

$$\epsilon(\omega, \mathbf{q}) = \epsilon_\infty - \frac{1}{q^2}\chi_0(\omega, \mathbf{q}), \tag{1}$$

with

$$\chi_0(\omega, \mathbf{q}) \propto \frac{1}{q^2} M^2 \int_{-\infty}^{\infty} \frac{F_k \Delta E}{\omega^2 - \Delta E^2 + i\Gamma_P \omega} d\mathbf{k}. \tag{2}$$

Here, $\Delta E = E_{\mathbf{k}+\mathbf{q}} - E_{\mathbf{k}}$, where $E_{\mathbf{k}}$ describes the band structure, $F_{\mathbf{k}}$ is the Fermi function, Γ_P is the lifetime broadening, and M is the matrix element. Using the complex dielectric function we then calculate the loss function $\mathrm{Im}[-1/\epsilon(\omega, \mathbf{q})]$. The maximum of the loss function as a function of momentum **q** which occurs at $\mathrm{Re}[\epsilon(\omega, \mathbf{q})] = \mathbf{0}$ yields the plasmon dispersion. In the calculation we use a constant matrix element, the absolute value being determined by the condition that the plasmon energy for $q = 0$ agrees with that derived from optical spectroscopy. The small momentum dependence of the matrix element is supported by the observation that for momentum $q \leqslant 0.5$ Å^{-1} the longitudinal f-sum rule [7] is reduced by less than 20%. Similar calculations were performed for polyacetylene [45], La_2CuO_4 [19], optimally doped $Bi_2Sr_2CaCu_2O_8$ [18,20], and for the ladder compound $Ca_xSr_{14-x}Cu_{24}O_{41}$ [22]. Interestingly, in all cases the low-energy dispersion could be well described using a simple *unrenormalized* tight-binding band structure.

In Sr_2RuO_4 the conduction band is composed of three Ru $4d$ t_{2g} bands, the narrow quasi-one-dimensional (1D) α/β bands, and the wider quasi-2D γ band, having, without taking into account the spin-orbit interaction, predominantly xz/yz and xy orbital character, respectively [34,39]. For the calculation of the plasmon dispersion we used an unrenormalized tight-binding band structure adjusted to an LDA band-structure calculation [41]. We obtain a minimum of the difference between the calculated and experimental plasmon dispersion by a shift of 0.2 eV of the band structure to lower binding energies. For calculations using Eq. (1) the neglect of the spin-orbit coupling is reasonable because the spin-orbit coupling is considerably smaller than the plasmon energy [39,46]. For the calculations we used the background dielectric function $\epsilon_\infty = 2.3$ from optical spectroscopy [29,30].

Using RPA for the homogeneous electron gas, the free-electron long-wavelength plasmon dispersion coefficient α [see Eq. (3)] is proportional to $v_{42} \propto \langle v_F^4 \rangle / \langle v_F^2 \rangle \approx \langle v_F^2 \rangle$ [20,44]. To control the anisotropy and orbital character of the calculated dispersions we have calculated v_{42} for the bands for **q** parallel to the [110] and [100] direction.

Results. In Fig. 1 we present the experimental loss spectra of Sr_2RuO_4 for momentum transfer parallel to the [110] and the [100] direction, measured at $T = 20$ K. At $T = 300$ K, within error bars, we obtain the same results. The strongest excitations occur between 1.5 and 1.8 eV, which are ascribed to plasmons of the charge carriers. At low energies, the intensity is dominated by the quasielastic peak. At higher energy near 3.3 eV, a small peak possibly due to interband transitions is visible at higher momentum transfer.

We derive a positive plasmon dispersion by an evaluation of the maxima of the loss data. In the long-wavelength limit the experimental and the calculated dispersion can be well described by

$$\omega(q) = \omega_p + \frac{\hbar^2}{m}\alpha q^2. \tag{3}$$

ω_p is equal to 1.49 eV which roughly agrees with the in-layer plasmon energy $\omega_p = 1.57$ eV derived from optical spectroscopy [26,29,30].

The dispersions of the plasmon along the two directions together with a fit for $q \leqslant 0.3$ Å^{-1} is depicted in Fig. 2. The derived dispersion coefficients are $\alpha_{110}^{\mathrm{expt}} = 0.22$ and $\alpha_{100}^{\mathrm{expt}} = 0.30$.

In this figure we have also added the calculated plasmon dispersion along the [110] and the [100] direction. The calculated dispersion coefficients for $q \leqslant 0.3$ Å^{-1} are $\alpha_{110}^{\mathrm{calc}} = 0.25$ and $\alpha_{100}^{\mathrm{calc}} = 0.21$. In Fig. 3 we present the plasmon width [full width at half maximum (FWHM)], derived from a fit of a Gaussian plus background to the loss data shown in Fig. 1. Along the two directions, within error bars the width is constant and equal to 0.7 eV up to $q = 0.4$ Å^{-1}. Above $q \approx 0.4$ Å^{-1} an increase of the plasmon width is detected.

Discussion. We have interpreted the principle excitation of the loss spectra near 1.5 eV by a charge carrier plasmon. Its finite width of 0.7 eV is smaller than the plasmon energy of 1.5 eV, indicating a quasiparticle excitation. The finite

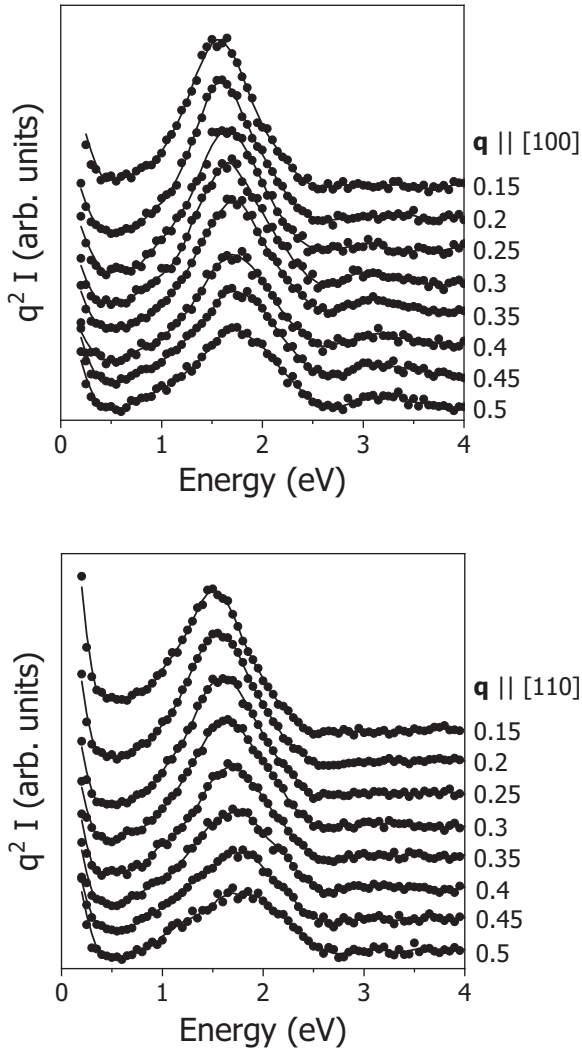

FIG. 1. Electron energy-loss spectra multiplied by q^2 (q^2I) of Sr_2RuO_4 in the energy range between 0 and 4 eV for momentum transfer **q** between 0.15 and 0.5 Å^{-1}. Upper panel: **q** parallel to the [100] direction; lower panel: **q** parallel to the [110] direction. Solid lines are guides to the eyes.

dispersion signals a propagating plasmon. We emphasize that the width is almost constant in the studied low momentum range. This means that it is not related to electron-electron interaction which would lead to a quadratic increase in momentum transfer [47]. The fact that the width is smaller than the energy signals that the excitation is not overdamped due to fluctuations in a quantum critical system, in contrast to theoretical predictions [6]. Rather, it is caused, as in most metallic systems, studied by T-EELS, by a decay into interband transitions [48–50]. These interbands are caused by a back-folding of bands from the second to the first Brillouin zone by a finite pseudopotential.

The observation of a nondispersing overdamped plasmon near 1.2 eV in the long-wavelength limit and a continuum for $q > 0.26$ Å^{-1} using R-EELS and T-EELS [31] is at variance with the present T-EELS results, showing a well-defined plasmon with a positive plasmon dispersion up to 0.45 Å^{-1}.

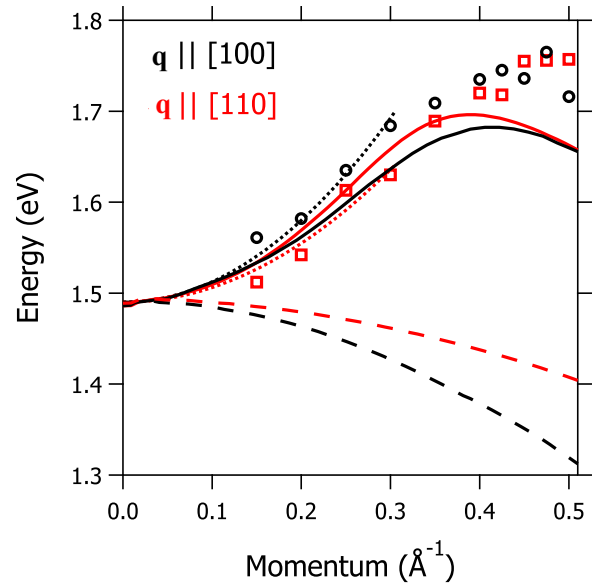

FIG. 2. Experimental data of the plasmon dispersion. Circles: Data for **q** parallel to [100]. Squares: Data for **q** parallel to [110]. Dotted line: Least-squares fit to the experimental data. Thick solid lines: Results from the calculations using an effective mass of one. All black data are for **q** parallel to [100]. The red (gray) data are for **q** parallel to [110]. Dashed lines: Calculations using an effective mass of four.

Looking at Fig. 2, the calculated plasmon dispersions, using an effective mass of one, are close to the experimental ones. On the other hand, the small experimental anisotropy is opposite to the calculated one. The difference between the experimental and the calculated dispersion may be explained by the distortion of the bands by a spin-orbit interaction [39],

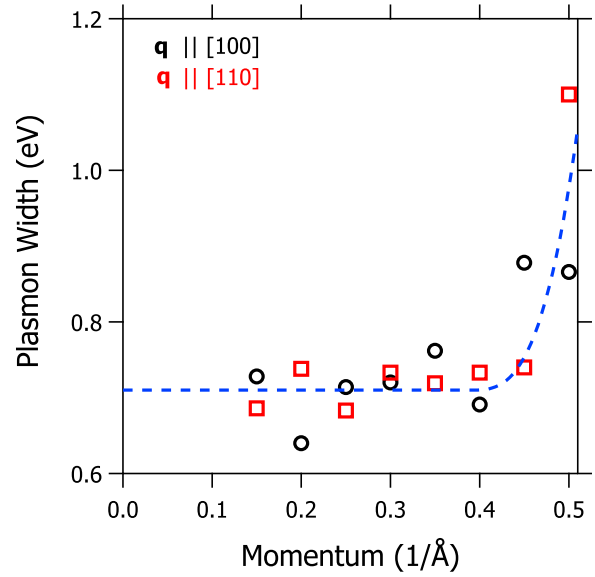

FIG. 3. Experimental data of the plasmon width as a function of momentum. Black circles: Data for **q** parallel to the [100] direction. Red (gray) squares: Data for **q** parallel to the [110] direction. The dashed line is a guide to the eyes.

not taken into account in our RPA calculations. An analysis of average Fermi velocities yields some information on the contribution of the three conduction bands to the plasmon dispersion: Along **q** parallel to the [110] directions, the dispersion is predominantly determined by the 2D γ band and to a lesser extent by the 1D α and β bands. Along the [100] direction, both the γ band and the α band contribute to the momentum dependence.

We emphasize that we obtain a qualitative agreement between the experimental and the calculated dispersion, although for this highly correlated system, we have used in the calculation an *unrenormalized* tight-binding band structure. The situation is similar to that in cuprates (see above) where the plasmon dispersion can be well described by RPA using an unrenormalized tight-binding band structure[18,20]. In the cuprates, where the band structure is renormalized by a factor of two, in the simplest approximation when the dispersion coefficient is proportional to the square of the Fermi velocity, one may expect a reduction of the plasmon dispersion due to flattening of the bands by a factor of 4. However, in Sr_2RuO_4 the average mass renormalization of the charge carrier is near 4.5 [39], which would lead in the above-mentioned approximation to a reduction of the plasmon dispersion by a factor of about 20. Actually, our RPA calculation using an effective mass $m^*/m = 4$ yields a negative plasmon dispersion (see Fig. 2). As explained in previous calculations [18,20], negative plasmon dispersion may occur because the dispersion coefficient is composed out of a positive and a negative contribution. A large reduction of the plasmon dispersion is not compatible with our experimental results. Thus our present results are clear proof that correlation effects do not influence the long-wavelength dispersion of the plasmon in systems which are correlated by the on-site Coulomb interaction in transition metal ions.

The weak influence of correlation effects on the plasmon dispersion can be rationalized by the following consideration. The dispersion is a measure of the compressibility of the electron liquid [7,44]. In the long-wavelength limit, the charge oscillations due to the plasmon excitation have a wavelength that is much larger than the distance between the next nearest Ru atoms. On the other hand, the mass enhancement in the correlated materials is predominantly caused by the hopping between neighboring transition metal atoms which is needed to overcome the on-site Coulomb interaction. In the long-wavelength limit of the plasmon excitations, the occupation number on the transition metal atoms is hardly changed and therefore the plasmon dispersion is not influenced by correlation effects. Moreover, at high energies, the mass enhancement is expected to be reduced [51] because the charge carriers are no longer coupled to spin excitations [3–5], which have an energy of the order of 100 meV. Furthermore, one can also understand the difference between EELS and ARPES studies. In the latter, the mass of a single hole is enhanced by an Auger-like valence band electron-hole excitation, leading in the final state to two holes in the occupied part of the band and therefore is influenced by the on-site Coulomb interaction.

Another indication of the nonsensitivity of the plasmon excitations to correlation effects is the plasmon width, being in the long-wavelength limit nearly independent of the momentum transfer (see Fig. 3). This demonstrates that in Sr_2RuO_4 the width is not caused by a lifetime broadening of the valence band due to a finite imaginary part of the self-energy, observed by ARPES. At $q = 0$ the plasmon width must be rigorously zero in a free-electron gas [13]. In the case of Al a quadratic momentum dependence of the width due to intraband particle-hole excitations was predicted by theoretical calculations [47], which is much too small compared to the experimental data of Al. Later, theoretical calculations [48,52] and experiments [50,53,54] showed that the plasmon width is predominantly caused by a decay of the plasmon into interband transitions related to back-folded bands from the second to the first Brillouin zone by a finite pseudopotential. This could lead to a constant or a negative q dependence of the plasmon width observed for $K_{0.3}MoO_3$ [54] or Li [53], respectively. Thus the constant width at low q in Sr_2RuO_4 is probably also caused by a decay into interband transitions and not by quantum critical fluctuations.

Moreover, there is also a more quantitative explanation of the differences of the imprint of correlation effects in ARPES and EELS studies, based on dynamical mean-field calculation theory [29,55]. These calculations predict for energies below about 0.1 eV a Fermi-liquid behavior with a mass enhancement of about four and above that energy a strongly reduced mass enhancement. This leads for the spectral function at low energies ($0.2 < \omega > -0.5$ eV) to a strongly renormalized dispersion and at higher energies to an unrenormalized dispersion of resilient quasiparticles which determine the "bad" metal properties. The observation of a plasmon dispersion, related to high-energy excitations, which are not influenced by correlation effects, is a clear indication of such resilient quasiparticles.

A comparison of the calculated susceptibility (not shown) and the plasmon dispersion shows that independent of the momentum direction, the plasmon merges into the single-particle excitations near $q = 0.4$ Å^{-1}. At this momentum also an additional broadening of the experimental plasmon width is observed (see Fig. 3). This behavior is very similar to that observed in nearly-free-electron metals [50].

There is a certain flattening of the experimental dispersion at higher momentum transfer. As it also appears in the RPA calculations, we conclude that it is not caused by correlation-induced local field corrections. Rather we infer that it is caused by the finite bandwidth of the conduction bands. To obtain information on the dynamic local field correction, experiments at higher momentum transfer are required.

In summary, we have observed in Sr_2RuO_4 a propagating plasmon, which is at low momentum and at high energies determined by resilient quasiparticles which are not renormalized. Extending future EELS measurements to higher momentum and into the low-energy range using an improved energy resolution will provide valuable information on the renormalized part of the spectral function and on the momentum dependence of correlation effects.

Acknowledgments. We thank P. Abbamonte, B. Büchner, L. Craco, S.-L. Drechsler, A. Lubk, and A. P. Mackenzie for helpful discussions, and M. Naumann for technical assistance. This work is supported by a KAKENHI Grants-in-Aids for Scientific Research (Grants No. 18K04715, No.

21H01033, and No. 22K19093), and Core-to-Core Program (No. JPJSCCA20170002) from the Japan Society for the Promotion of Science (JSPS) and by a JST-Mirai Program (Grant No. JPMJMI18A3).

[1] A. Damascelli, Z. Hussain, and Z.-X. Shen, Rev. Mod. Phys. **75**, 473 (2003).
[2] N. M. Plakida, Phys. C: Superconductivity. **531**, 39 (2016).
[3] T. Tohyama, P. Horsch, and S. Maekawa, Phys. Rev. Lett. **74**, 980 (1995).
[4] G. Khaliullin and P. Horsch, Phys. Rev. B **54**, R9600(R) (1996).
[5] R. Eder, Y. Ohta, and S. Maekawa, Phys. Rev. Lett. **74**, 5124 (1995).
[6] A. Romero-Bermúdez, A. Krikun, K. Schalm, and J. Zaanen, Phys. Rev. B **99**, 235149 (2019).
[7] G. D. Mahan, *Many-Particle Physics* (Kluwer Academic/Plenum, New York, 2000).
[8] S. Vig, A. Kogar, M. Mitrano, A. Husain, L. Venema, M. Rak, V. Mishra, P. Johnson, G. Gu, E. Fradkin, M. Norman, and P. Abbamonte, SciPost Phys. **3**, 026 (2017).
[9] M. Mitrano, A. A. Husain, S. Vig, A. Kogar, M. S. Rak, S. I. Rubeck, J. Schmalian, B. Uchoa, J. Schneeloch, R. Zhong, G. D. Gu, and P. Abbamonte, Proc. Natl. Acad. Sci. USA **115**, 5392 (2018).
[10] A. A. Husain, M. Mitrano, M. S. Rak, S. Rubeck, B. Uchoa, K. March, C. Dwyer, J. Schneeloch, R. Zhong, G. D. Gu, and P. Abbamonte, Phys. Rev. X **9**, 041062 (2019).
[11] H. Raether, in *Springer Tracts in Modern Physics*, edited by G. Höhler (Springer, Berlin, 1965), Vol. 38, p. 85.
[12] J. Daniels, C. von Festenberg, H. Raether, and K. Zeppenfeld, in *Springer Tracts in Modern Physics*, edited by G. Höhler (Springer, Berlin, 1970), Vol. 54, p. 77.
[13] J. Schnatterly, Solid State Phys. **34**, 275 (1979).
[14] P. Schattschneider, *Fundamentals of Inelastic Electron Scattering* (Springer, Wien, 1986).
[15] J. Fink, Adv. Electron. Electron Phys. **75**, 121 (1989).
[16] F. Roth, A. König, J. Fink, B. Büchner, and M. Knupfer, J. Electron Spectrosc. Relat. Phenom. **195**, 85 (2014).
[17] N. Nücker, H. Romberg, S. Nakai, B. Scheerer, J. Fink, Y. F. Yan, and Z. X. Zhao, Phys. Rev. B **39**, 12379 (1989).
[18] N. Nücker, U. Eckern, J. Fink, and P. Müller, Phys. Rev. B **44**, 7155 (1991).
[19] G. Vielsack and R. von Baltz, Phys. Status Solidi B **158**, 249 (1990).
[20] V. G. Grigoryan, G. Paasch, and S.-L. Drechsler, Phys. Rev. B **60**, 1340 (1999).
[21] G. Paasch and V. G. Grigoryan, Ukr. J. Phys. **44**, 1480 (1999).
[22] F. Roth, A. Revcolevschi, B. Büchner, M. Knupfer, and J. Fink, Phys. Rev. B **101**, 195132 (2020).
[23] Y. Maeno, H. Hashimoto, K. Yoshida, S. Nishizaki, T. Fujita, J. G. Bednorz, and F. Lichtenberg, Nature (London) **372**, 532 (1994).
[24] A. P. Mackenzie and Y. Maeno, Rev. Mod. Phys. **75**, 657 (2003).
[25] R. Sharma, S. D. Edkins, Z. Wang, A. Kostin, C. Sow, Y. Maeno, A. P. Mackenzie, J. C. S. Davis, and V. Madhavan, Proc. Natl. Acad. Sci. USA **117**, 5222 (2020).
[26] T. Katsufuji, M. Kasai, and Y. Tokura, Phys. Rev. Lett. **76**, 126 (1996).
[27] M. G. Hildebrand, M. Reedyk, T. Katsufuji, and Y. Tokura, Phys. Rev. Lett. **87**, 227002 (2001).
[28] K. Pucher, A. Loidl, N. Kikugawa, and Y. Maeno, Phys. Rev. B **68**, 214502 (2003).
[29] D. Stricker, J. Mravlje, C. Berthod, R. Fittipaldi, A. Vecchione, A. Georges, and D. van der Marel, Phys. Rev. Lett. **113**, 087404 (2014).
[30] D. Stricker, Ph.D. thesis, University Geneve, 2015.
[31] A. A. Husain, M. Mitrano, M. S. Rak, S. I. Rubeck, H. Yang, C. Sow, Y. Maeno, P. E. Batson, and P. Abbamonte, arXiv:2007.06670.
[32] Z. Wang, D. Walkup, P. Derry, T. Scaffidi, M. Rak, S. Vig, A. Kogar, I. Zeljkovic, A. Husain, L. H. Santos, Y. Wang, A. Damascelli, Y. Maeno, P. Abbamonte, E. Fradkin, and V. Madhavan, Nat. Phys. **13**, 799 (2017).
[33] S.-C. Wang, H.-B. Yang, A. K. P. Sekharan, H. Ding, J. R. Engelbrecht, X. Dai, Z. Wang, A. Kaminski, T. Valla, T. Kidd, A. V. Fedorov, and P. D. Johnson, Phys. Rev. Lett. **92**, 137002 (2004).
[34] N. J. C. Ingle, K. M. Shen, F. Baumberger, W. Meevasana, D. H. Lu, Z.-X. Shen, A. Damascelli, S. Nakatsuji, Z. Q. Mao, Y. Maeno, T. Kimura, and Y. Tokura, Phys. Rev. B **72**, 205114 (2005).
[35] M. W. Haverkort, I. S. Elfimov, L. H. Tjeng, G. A. Sawatzky, and A. Damascelli, Phys. Rev. Lett. **101**, 026406 (2008).
[36] V. B. Zabolotnyy, D. V. Evtushinsky, A. A. Kordyuk, T. K. Kim, E. Carleschi, B. P. Doyle, R. Fittipaldi, M. Cuoco, A. Vecchione, and S. V. Borisenko, J. Electron Spectrosc. Relat. Phenom. **191**, 48 (2013).
[37] C. N. Veenstra, Z.-H. Zhu, M. Raichle, B. M. Ludbrook, A. Nicolaou, B. Slomski, G. Landolt, S. Kittaka, Y. Maeno, J. H. Dil, I. S. Elfimov, M. W. Haverkort, and A. Damascelli, Phys. Rev. Lett. **112**, 127002 (2014).
[38] S. Akebi, T. Kondo, M. Nakayama, K. Kuroda, S. Kunisada, H. Taniguchi, Y. Maeno, and S. Shin, Phys. Rev. B **99**, 081108(R) (2019).
[39] A. Tamai, M. Zingl, E. Rozbicki, E. Cappelli, S. Riccó, A. de la Torre, S. McKeown Walker, F. Y. Bruno, P. D. C. King, W. Meevasana, M. Shi, M. Radović, N. C. Plumb, A. S. Gibbs, A. P. Mackenzie, C. Berthod, H. U. R. Strand, M. Kim, A. Georges, and F. Baumberger, Phys. Rev. X **9**, 021048 (2019).
[40] D. J. Singh, Phys. Rev. B **52**, 1358 (1995).
[41] A. Liebsch and A. Lichtenstein, Phys. Rev. Lett. **84**, 1591 (2000).
[42] J. S. Bobowski, N. Kikugawa, T. Miyoshi, H. Suwa, H. shu Xu, S. Yonezawa, D. A. Sokolov, A. P. Mackenzie, and Y. Maeno, Condensed Matter **4**, 6 (2019).
[43] H. Ehrenreich and M. H. Cohen, Phys. Rev. **115**, 786 (1959).
[44] G. F. Giuliani and G. Vignale, *Quantum Theory of the Electron Liquid* (Cambridge University Press, Cambridge, UK, 2005).
[45] C.-S. Neumann and R. von Baltz, Phys. Rev. B **35**, 9708 (1987).

[46] Z. V. Pchelkina, I. A. Nekrasov, T. Pruschke, A. Sekiyama, S. Suga, V. I. Anisimov, and D. Vollhardt, Phys. Rev. B **75**, 035122 (2007).
[47] D. F. DuBois and M. G. Kivelson, Phys. Rev. **186**, 409 (1969).
[48] G. Paasch, Phys. Status Solidi B **38**, A123 (1970).
[49] P. C. Gibbons, S. E. Schnatterly, J. J. Ritsko, and J. R. Fields, Phys. Rev. B **13**, 2451 (1976).
[50] A. vom Felde, J. Sprösser-Prou, and J. Fink, Phys. Rev. B **40**, 10181 (1989).
[51] J. Fink, Europhys. Lett. **113**, 27002 (2016).
[52] K. Sturm and L. E. Oliveira, Phys. Rev. B **40**, 3672 (1989).
[53] P. C. Gibbons and S. E. Schnatterly, Phys. Rev. B **15**, 2420 (1977).
[54] M. Sing, V. G. Grigoryan, G. Paasch, M. Knupfer, J. Fink, B. Lommel, and W. Aßmus, Phys. Rev. B **59**, 5414 (1999).
[55] X. Deng, J. Mravlje, R. Žitko, M. Ferrero, G. Kotliar, and A. Georges, Phys. Rev. Lett. **110**, 086401 (2013).